37

PRECONDITIONING IN THE PATH-FOLLOWING ALGORITHM FOR THE STOKES FLOW WITH STICK-SLIP CONDITIONS

37.1 INTRODUCTION

The paper deals with the Stokes flow with the stick-slip boundary conditions. Unlike the classical Navier law [1], we consider the case when the slip of a fluid along the wall may occur only when the shear stress attains certain bound which is given a-priori and does not depend on the solution itself. The mathematical model of the velocity-pressure formulation leads to the so-called variational inequality of the second kind. This problem exhibits many attractive applications: blood flow, metal forming processes, the polymer flow, or the hydrodynamics problems; see [2, 3] and references therein.

Our approximation uses the mixed finite element method based on the P1-bubble/P1 finite element pair [4]. The stiffness matrices are generated by a vectorized code [5]. The finite element approximation is combined with the TFETI domain decomposition method [6]. The dual algebraic problem arising after the elimination of the velocity and the pressure components leads to the minimization of the quadratic, strictly convex function in terms of three Lagrange multipliers representing: the gluing condition (including the Dirichlet boundary condition), the impermeability condition on the slip part of the boundary and the stick-slip condition. The third Lagrange multiplier is subject to box constraints and, due to the use of the TFETI method, all Lagrange multipliers have to satisfy a linear equality constraint. The solution to the dual problem is computed by a path-following variant of the interior-point method [7] adapted for the box and the linear equality constraints [8]. Highly promising numerical experiments of the path-following algorithm for non-decomposed problems has been presented in [9]. However, an extension of the algorithm for the TFETI is non-trivial.

The main idea of the algorithm consists on the use of the damped Newton method whose iterations lay in a neighborhood of a central path leading to the solution. The inner subproblems are given by linear systems with a block structure. These systems are reduced using the Schur complement method so that a variant of the preconditioned projected conjugate gradient method (PPCGM) may be used. The PPCGM generates iterations in a subspace determined by the kernel of the matrix representing the dual equality constraints. An appropriate preconditioner eliminates ill conditioning of the reduced systems that arises typically in interior point methods when the iterations approach the solution. For thet, we use the oblique projector. Our numerical experiments are performed by the decomposed problems taken from [9]. The first results computed with the TFETI active set strategy algorithm and a brief description of the simplified version of the TFETI path-following algorithm could be found in [10]. The main issue of this paper is an experimental assessments of the quality of the preconditioning variants that arise from the spectral analysis of the preconditioning technique [8].

37.2 FORMULATION OF THE PROBLEM

Let Ω be a bounded domain in $\mathbb{R}^2$ whose sufficiently smooth boundary $\partial\Omega$ is split into three non-empty disjoint parts: $\partial\Omega = \overline{\gamma}_D \cup \overline{\gamma}_N \cup \overline{\gamma}_C$. We consider the model of a viscous incompressible Newtonian fluid modelled by the Stokes system with the Dirichlet and Neumann boundary conditions on γ_D and γ_N, respectively, and with the impermeability and the stick-slip boundary condition of the Tresca type on γ_C:

$$\left.\begin{array}{rcll} -\eta\Delta\boldsymbol{u} + \nabla p &=& \boldsymbol{f} & \text{in } \Omega, \\ \nabla\cdot\boldsymbol{u} &=& 0 & \text{in } \Omega, \\ \boldsymbol{u} &=& \boldsymbol{u}_D & \text{on } \gamma_D, \\ \boldsymbol{\sigma} &=& \boldsymbol{\sigma}_N & \text{on } \gamma_N, \\ |\sigma_t(\boldsymbol{x})| < g(\boldsymbol{x}) \;\Rightarrow\; u_t(\boldsymbol{x}) &=& 0 & \boldsymbol{x}\in\gamma_C, \\ |\sigma_t(\boldsymbol{x})| = g(\boldsymbol{x}) \;\Rightarrow\; \exists\kappa(\boldsymbol{x})\geq 0 : \sigma_t(\boldsymbol{x}) &=& -\kappa(\boldsymbol{x})u_t(\boldsymbol{x}) & \boldsymbol{x}\in\gamma_C, \end{array}\right\} \tag{37.1}$$

where $\boldsymbol{\sigma} = \eta\partial\boldsymbol{u}/\partial\boldsymbol{n} - p\boldsymbol{n}$. Here, $\boldsymbol{u} = (u_1, u_2)$ is the flow velocity, p is the pressure, $\boldsymbol{f} = (f_1, f_2)$ represents forces acting on the fluid, $\eta > 0$ is the dynamic viscosity, and $\boldsymbol{u}_D$, $\boldsymbol{\sigma}_N$ are the given Dirichlet and Neumann boundary data, respectively. Further $\boldsymbol{n} = (n_1, n_2)$, $\boldsymbol{t} = (-n_2, n_1)$ is the unit outward normal and tangential vector to $\partial\Omega$, respectively, while $u_n = \boldsymbol{u}\cdot\boldsymbol{n}$, $u_t = \boldsymbol{u}\cdot\boldsymbol{t}$ is the normal and tangential component of $\boldsymbol{u}$ along $\partial\Omega$, respectively. Finally $\sigma_t = \boldsymbol{\sigma}\cdot\boldsymbol{t}$ is the shear stress and $g \geq 0$ is a given slip bound function on γ_C. Further we decompose Ω into s non-overlapping subdomains Ω_i such that $\overline{\Omega} = \bigcup_{i=1}^{s}\overline{\Omega}_i$.

The dual algebraic problem reads as follows:

$$\textit{Find } \boldsymbol{\lambda}\in\boldsymbol{\Lambda} \textit{ such that } \; q(\boldsymbol{\lambda}) \leq q(\boldsymbol{\mu}) \quad \forall\boldsymbol{\mu}\in\boldsymbol{\Lambda} \tag{37.2}$$

with $q : \boldsymbol{\Lambda}\to\mathbb{R}$, $q(\boldsymbol{\mu}) = \frac{1}{2}\boldsymbol{\mu}^T\mathbf{F}\boldsymbol{\mu} - \boldsymbol{\mu}^T\mathbf{d}$ and $\boldsymbol{\Lambda} = \{\boldsymbol{\mu} = (\boldsymbol{\mu}_e^T, \boldsymbol{\mu}_n^T, \boldsymbol{\mu}_t^T)^T : |\boldsymbol{\mu}_t| \leq \mathbf{g}, \mathbf{G}\boldsymbol{\mu} = \mathbf{e}\}$,

where $\mathbf{F} = \mathbf{C}\mathbf{M}^{+}\mathbf{C}^{T}$, $\mathbf{d} = \mathbf{C}\mathbf{M}^{+}\mathbf{f} - \bar{\mathbf{u}}_D$, $\mathbf{G} = -\mathbf{R}^{T}\mathbf{C}^{T}$, $\mathbf{e} = -\mathbf{R}^{T}\mathbf{f}$, and

$$\mathbf{M} = \begin{pmatrix} \mathbf{A} & \mathbf{B}^{T} \\ \mathbf{B} & -\mathbf{E} \end{pmatrix}, \ \mathbf{f} = \begin{pmatrix} \mathbf{f}_u \\ \mathbf{c} \end{pmatrix}, \ \mathbf{C} = \begin{pmatrix} \mathbf{B}_e \\ \mathbf{N} \\ \mathbf{T} \end{pmatrix}, \ \bar{\mathbf{u}}_D = \begin{pmatrix} \mathbf{u}_D \\ \mathbf{0} \\ \mathbf{0} \end{pmatrix}.$$

Some of the objects exhibit a block structure due to the TFETI method that can be used for a parallel implementation. The stiffness matrix for the Laplace operator is $\mathbf{A} = \mathrm{diag}(\mathbf{A}_1, \ldots, \mathbf{A}_s)$ with symmetric, positive semidefinite blocks of defect two, $\mathbf{f}_u = (\mathbf{f}_{u1}^{T}, \ldots, \mathbf{f}_{us}^{T})^{T}$ represents nodal forces, the stiffness matrix for the divergence operator is $\mathbf{B} = \mathrm{diag}(\mathbf{B}_1, \ldots, \mathbf{B}_s)$ with full row-rank blocks. The matrix and the vector arising from the elimination of the bubble components are $\mathbf{E} = \mathrm{diag}(\mathbf{E}_1, \ldots, \mathbf{E}_s)$ with symmetric, positive semidefinite blocks and $\mathbf{c} = (\mathbf{c}_1^{T}, \ldots, \mathbf{c}_s^{T})^{T}$. The matrix $\mathbf{B}_e$ enforces the continuity of the solution and ensures the Dirichlet boundary condition. The Dirichlet data are placed in $\mathbf{u}_D$. The i-th row of $\mathbf{N}, \mathbf{T}$ is defined by the normal vector $\boldsymbol{n}(\boldsymbol{x}_i)$, the tangential vector $\boldsymbol{t}(\boldsymbol{x}_i)$, respectively, where $\boldsymbol{x}_i$ is the node belonging to $\overline{\gamma}_C \setminus \overline{\gamma}_D$. The redundancy is eliminated so that $\mathbf{C}$ has full row rank. The vector $\mathbf{g}$ collects the slip bound values at the nodes $\boldsymbol{x}_i \in \overline{\gamma}_C \setminus \overline{\gamma}_D$ (arising from a numerical integration of q). The null space basis to $\mathbf{M}$ may by assembled as follows:

$$\mathbf{R}_{A_i} = \begin{pmatrix} \mathbf{1} & \mathbf{0} \\ \mathbf{0} & \mathbf{1} \end{pmatrix}, \quad \mathbf{R}_A = \mathrm{diag}(\mathbf{R}_{A_1}, \ldots, \mathbf{R}_{A_s}), \quad \mathbf{R} = \begin{pmatrix} \mathbf{R}_A \\ \mathbf{0} \end{pmatrix},$$

where $\mathbf{1}$ is the vector of all ones.

After obtaining $\boldsymbol{\lambda}$ from (37.2), one compute the velocity and the pressure components using $\mathbf{w} = \mathbf{M}^{+}(\mathbf{f} - \mathbf{C}^{T}\boldsymbol{\lambda}) + \mathbf{R}\boldsymbol{\alpha}$, where $\boldsymbol{\alpha}$ is also result of the solution method for (37.2) and $\mathbf{w} = (\mathbf{u}_1^{T}, \mathbf{p}_1^{T}, \ldots, \mathbf{u}_s^{T}, \mathbf{p}_s^{T})^{T}$. The actions of the generalized inverse $\mathbf{M}^{+}$ to $\mathbf{M}$ can be computed by the method introduced in [11].

37.3 PATH-FOLLOWING ALGORITHM

The starting point for the algorithm is the constrained equation that is equivalent to the Karush-Kuhn-Tucker optimality conditions to (37.2) [8]:

$$\mathbf{H}(\mathbf{v}) = \mathbf{0}, \ \boldsymbol{\nu} \geq \mathbf{0}, \ \mathbf{z} \geq \mathbf{0}, \tag{37.3}$$

where

$$\mathbf{H}(\mathbf{v}) = \begin{pmatrix} \mathbf{F}\boldsymbol{\lambda} - \mathbf{d} + \mathbf{G}^{T}\boldsymbol{\mu} + \begin{pmatrix} -\boldsymbol{\nu}_1 + \boldsymbol{\nu}_2 \\ \mathbf{0} \end{pmatrix} \\ \mathbf{G}\boldsymbol{\lambda} - \mathbf{e} \\ \begin{pmatrix} -\boldsymbol{\lambda}_t - \mathbf{g} \\ \boldsymbol{\lambda}_t - \mathbf{g} \end{pmatrix} + \mathbf{z} \\ \mathbf{NZ1} \end{pmatrix}, \tag{37.4}$$

with $\mathbf{v} = (\boldsymbol{\lambda}^T, \boldsymbol{\mu}^T, \boldsymbol{\nu}^T, \mathbf{z}^T)^T$, $\boldsymbol{\nu} = (\boldsymbol{\nu}_1^T, \boldsymbol{\nu}_2^T)^T$, $\mathbf{N} = \mathrm{diag}(\boldsymbol{\nu})$, $\mathbf{Z} = \mathrm{diag}(\mathbf{z})$, and $\mathbf{1}$ is the vector of all ones. The problem (37.3) is solved by the Newton-type method so that the non-singular Jacobi matrix $\mathbf{J} = \mathbf{J}(\mathbf{v})$ to $\mathbf{H}$ is needed. It is the matrix of the linear system (37.5) with $\mathbf{J}_{13} = \mathbf{J}_{31}^T = \begin{pmatrix} -\mathbf{I} & \mathbf{I} \\ \mathbf{0} & \mathbf{0} \end{pmatrix}$. Since $\mathbf{z}$ is always positive, $\mathbf{J}(\mathbf{v})$ is non-singular for any $\boldsymbol{\nu} \geq \mathbf{0}$. The path-following algorithm exploit a damping procedure keeping the Newton iterations near the so-called central path tending the solution proportionally. It allows that longer steps may be performed; see [8] for more details. Another key of the computational efficiency is the way how the inner linear systems are solved.

37.4 PRECONDITIONING OF INNER LINEAR SYSTEMS

The inner linear systems read as follows:

$$\begin{pmatrix} \mathbf{F} & \mathbf{G}^T & \mathbf{J}_{13} & \mathbf{0} \\ \mathbf{G} & \mathbf{0} & \mathbf{0} & \mathbf{0} \\ \mathbf{J}_{31} & \mathbf{0} & \mathbf{0} & \mathbf{I} \\ \mathbf{0} & \mathbf{0} & \mathbf{Z} & \mathbf{N} \end{pmatrix} \begin{pmatrix} \Delta\mathbf{x} \\ \Delta\boldsymbol{\mu} \\ \Delta\boldsymbol{\nu} \\ \Delta\mathbf{z} \end{pmatrix} = \begin{pmatrix} \mathbf{r}_1 \\ \mathbf{r}_2 \\ \mathbf{r}_3 \\ \mathbf{r}_4 \end{pmatrix}, \tag{37.5}$$

where $\mathbf{r}_1$, $\mathbf{r}_2 = \mathbf{0}$, $\mathbf{r}_3, \mathbf{r}_4$ stand for the components of the right-hand side vector. For solving (37.5) we use the Schur complement reduction. From the third and the fourth block equations in (37.5), we get $\Delta\mathbf{z} = \mathbf{r}_3 - \mathbf{J}_{31}\Delta\mathbf{x}$ and $\Delta\boldsymbol{\nu} = \mathbf{Z}^{-1}(\mathbf{r}_4 - \mathbf{N}\mathbf{r}_3) + \mathbf{Z}^{-1}\mathbf{N}\mathbf{J}_{31}\Delta\mathbf{x}$, respectively. The reduced system for unknows $\Delta\mathbf{x}$ and $\Delta\boldsymbol{\mu}$ takes the form

$$\begin{pmatrix} \bar{\mathbf{F}} & \mathbf{G}^T \\ \mathbf{G} & \mathbf{0} \end{pmatrix} \begin{pmatrix} \Delta\mathbf{x} \\ \Delta\boldsymbol{\mu} \end{pmatrix} = \begin{pmatrix} \bar{\mathbf{r}}_\mathbf{1} \\ \mathbf{0} \end{pmatrix}, \tag{37.6}$$

where $\bar{\mathbf{F}} = \mathbf{F} + \mathbf{D}$, $\mathbf{D} = \mathrm{diag}(\mathbf{Z}_1^{-1}\mathbf{N}_1 + \mathbf{Z}_2^{-1}\mathbf{N}_2, \mathbf{0})$ is diagonal with $\mathbf{N}_i = \mathrm{diag}(\boldsymbol{\nu}_i)$, $\mathbf{Z}_i = \mathrm{diag}(\mathbf{z}_i)$, $i = 1, 2$, $\mathbf{z} = (\mathbf{z}_1^T, \mathbf{z}_2^T)^T$, and $\bar{\mathbf{r}}_\mathbf{1} = \mathbf{r}_1 + \mathbf{J}_{13}\mathbf{Z}^{-1}(\mathbf{N}\mathbf{r}_3 - \mathbf{r}_4)$. The matrices $\bar{\mathbf{F}}$ and $\mathbf{D}$ are symmetric, positive semidefinite but they may be singular.

The second equation in (37.6) yields that $\Delta\mathbf{x} \in \mathit{Ker}\,\mathbf{G}$. Let us introduce the *orthogonal projector* onto $\mathit{Ker}\,\mathbf{G}$ defined by $\mathbf{P} = \mathbf{I} - \mathbf{G}^T(\mathbf{G}\mathbf{G}^T)^{-1}\mathbf{G}$. Multiplying the first equation in (37.6) by $\mathbf{P}$, we arrive at the projected equation

$$\mathbf{P}\bar{\mathbf{F}}\Delta\mathbf{x} = \mathbf{P}\bar{\mathbf{r}}_\mathbf{1}, \quad \Delta\mathbf{x} \in \mathit{Ker}\,\mathbf{G}. \tag{37.7}$$

The invertibility of $\mathbf{P}\bar{\mathbf{F}}$ on $\mathit{Ker}\,\mathbf{G}$ is guaranteed [8] so that the unique solution to (37.7) may be computed by the projected conjugate gradient method. The unknown $\Delta\boldsymbol{\mu}$ in (37.6) is computed, after obtaining $\Delta\mathbf{x}$, by $\Delta\boldsymbol{\mu} = (\mathbf{G}\mathbf{G}^T)^{-1}\mathbf{G}(\bar{\mathbf{r}}_1 - \bar{\mathbf{F}}\Delta\mathbf{x})$.

The equation (37.7) requires an efficient preconditiong, since the diagonal entries of $\mathbf{D}$ tend to infinity for components of $\mathbf{z} \geq \mathbf{0}$ in (37.3) that are satisfied as equality. We will use the preconditioner $\mathbf{P}\bar{\mathbf{D}}$ with $\bar{\mathbf{D}} = \mathbf{D}_F + \mathbf{D}$, where $\mathbf{D}_F$ is an appropriate symmetric, positive definite matrix. The preconditioned variant of (37.7) is the projected equation

$$[\mathbf{P}\bar{\mathbf{D}}]^{-1}\mathbf{P}\bar{\mathbf{F}}\Delta\mathbf{x} = [\mathbf{P}\bar{\mathbf{D}}]^{-1}\mathbf{P}\bar{\mathbf{r}}_\mathbf{1}, \quad \Delta\mathbf{x} \in \mathit{Ker}\,\mathbf{G}, \tag{37.8}$$

where $[\mathbf{P}\bar{\mathbf{D}}]^{-1}$ denotes the inverse to $\mathbf{P}\bar{\mathbf{D}}$ on *Ker* $\mathbf{G}$. This inverse can be computed by the formula

$$[\mathbf{P}\bar{\mathbf{D}}]^{-1} = \mathbf{P}_{\bar{\mathbf{D}}^{-1}}\bar{\mathbf{D}}^{-1},$$

where $\mathbf{P}_{\bar{\mathbf{D}}^{-1}} = \mathbf{I} - \bar{\mathbf{D}}^{-1}\mathbf{G}^T(\mathbf{G}\bar{\mathbf{D}}^{-1}\mathbf{G}^T)^{-1}\mathbf{G}$ is the oblique projector onto *Ker* $\mathbf{G}$.

The equation (37.8) can be solved by the PPCGM. The convergence depends on the spectrum of $[\mathbf{P}\bar{\mathbf{D}}]^{-1}\mathbf{P}\bar{\mathbf{F}}$ on *Ker* $\mathbf{G}$. Let $f_{\min}$, $f_{\max}$ be the smallest, largest eigenvalue to $\mathbf{F}$ on *Ker* $\mathbf{G}$, respectively, and let $d_{\min}$, $d_{\max}$ be the smallest, largest eigenvalue to $\mathbf{D}_F$ on *Ker* $\mathbf{G}$, respectively. The following result holds [8] .

Theorem 37.1 *The eigenvalues* λ *of* $[\mathbf{P}\bar{\mathbf{D}}]^{-1}\mathbf{P}\bar{\mathbf{F}}$ *on Ker* $\mathbf{G}$ *satisfy:*

(i) if $f_{\min} < d_{\max}$ *and* $d_{\min} < f_{\max}$*, then* $\lambda \in [f_{\min}d_{\max}^{-1}, f_{\max}d_{\min}^{-1}]$*;*

(ii) if $d_{\max} \leq f_{\min}$*, then* $\lambda \in [1, f_{\max}d_{\min}^{-1}]$*;*

(iii) if $f_{\max} \leq d_{\min}$*, then* $\lambda \in [f_{\min}d_{\max}^{-1}, 1]$.

As the consequence we get the bounds on the spectral condition number κ of the preconditioned, projected operator on *Ker* $\mathbf{G}$.

Corollary 37.1 *Theorem 37.1 implies:*

(i) if $f_{\min} < d_{\max}$ *and* $d_{\min} < f_{\max}$*, then* $\kappa([\mathbf{P}\bar{\mathbf{D}}]^{-1}\mathbf{P}\bar{\mathbf{F}}) \leq \kappa(\mathbf{F})\kappa(\mathbf{D}_F)$*;*

(ii) if $d_{\max} \leq f_{\min}$*, then* $\kappa([\mathbf{P}\bar{\mathbf{D}}]^{-1}\mathbf{P}\bar{\mathbf{F}}) \leq f_{\max}/d_{\min}$*;*

(iii) if $f_{\max} \leq d_{\min}$*, then* $\kappa([\mathbf{P}\bar{\mathbf{D}}]^{-1}\mathbf{P}\bar{\mathbf{F}}) \leq d_{\max}/f_{\min}$.

The efficiency of precoditioning will be tested experimentally.

37.5 NUMERICAL EXPERIMENTS

Let $\Omega = (0,1) \times (0,1)$, $\gamma_D = (0,1) \times \{1\}$, $\gamma_{N_{left}} = \{0\} \times (0,1)$, $\gamma_{N_{right}} = \{1\} \times (0,1)$, $\gamma_N = \gamma_{N_{left}} \cup \gamma_{N_{right}}$, and $\gamma_C = \{(x, 0.8(x - x^2)) : x \in (0,1)\}$. The data of problem (37.1) are defined as follows: $\boldsymbol{f} = -\nu\Delta\boldsymbol{u}_{exp} + \nabla \mathtt{p}_{exp}$, $\nu = 1$, $\boldsymbol{u}_D = \mathbf{0}$, $\boldsymbol{\sigma}_N = \boldsymbol{\sigma}_{exp|_{\gamma_N}}$, and $g = 10$, where $\boldsymbol{u}_{exp}(x,y) = (-\cos(2\pi x)\sin(2\pi y) + \sin(2\pi y), \sin(2\pi x)\cos(2\pi y) - \sin(2\pi x))$ and $p_{exp}(x,y) = 2\pi(\cos(2\pi y) - \cos(2\pi x))$. Note that $\boldsymbol{u}_{exp}$ and p_{exp} do not solve (37.1). The finite element mesh, the velocity, and the pressure field are drawn in Figure 37.1. On γ_C we prescribe different values of g in order to illustrate friction effects that are seen in Figure 37.2 for slip boundary. All results are calculated by the terminating tolerance $tol = 10^{-5}$ for the path-following algorithm. All codes are implemented in Matlab 2013b. The computations were performed by ANSELM supercomputer at IT4I VŠB-TU Ostrava.

In tables below we introduce complexity of computations in terms of matrix-vector multiplications by $\mathbf{F}$ (boldface numbers) for different numbers of subdomains (s), *primal* unknowns ($3n$, where n is the number of finite element nodes over all subdomanis), and

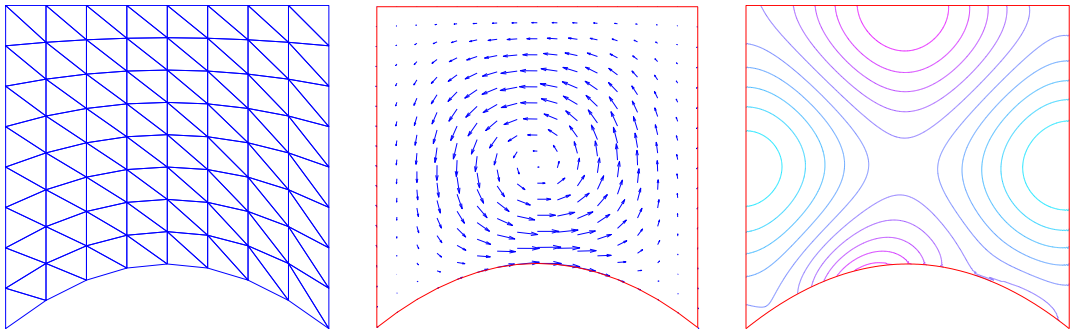

Fig. 37.1 $g = 10$**: mesh (left), velocity field (middle), isobars (right)**
Source: own elaboration

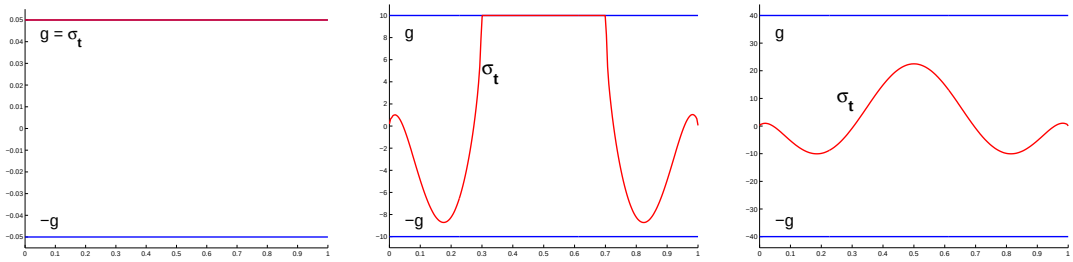

Fig. 37.2 $g = 0.05$ **(left),** $g = 10$ **(middle),** $g = 40$ **(right)**
Source: own elaboration

dual unknowns ($3n_e + 2n_d + 2n_c$, where n_e is the number of nodes in which gluing of subdomain solutions is required, n_d is the number of nodes in which the Dirichlet boundary condition is prescribed, and n_c is the number of nodes on the slip part of the boundary). We denote by h and H the norm (diameter) of the finite element triangles and the subdomains, respectively.

Example 1. We test the efficiency of the preconditioners with the fixed ratio $H/h = 8$. In Table 37.1–Table 37.4 we use $\mathbf{D}_F = \mathbf{I}$, $\mathbf{D}_F = d \times \mathbf{I}$ with $d = (f_{\max} + f^+_{\min})/2$ (where $f^+_{\min}$ is the smallest positive eigenvalue of $\mathbf{F}$), $\mathbf{D}_F = abs(diag(\mathbf{F}))$, and $\mathbf{D}_F = diag(\mathbf{F})$, respectively. The best performance is achieved for the last case.

Tab. 37.1 $\mathbf{D}_F = \mathbf{I}$

s	$primal/dual$	$g = 0.05$	$g = 10$	$g = 40$
$4(2 \times 2)$	972/173	**536**	**631**	**648**
$16(4 \times 4)$	3888/753	**717**	**1205**	**1292**
$36(6 \times 6)$	8748/1741	**850**	**1390**	**1254**
$64(8 \times 8)$	15552/3137	**979**	**1419**	**1858**
$100(10 \times 10)$	24300/4941	**1386**	**1643**	**1917**

Source: own elaboration

Tab. 37.2 $\mathbf{D}_F = d \times \mathbf{I}$ **with** $d = (f_{\max} + f^+_{\min})/2$

s	$primal/dual$	$g = 0.05$	$g = 10$	$g = 40$
$4(2 \times 2)$	972/173	**434**	**620**	**636**
$16(4 \times 4)$	3888/753	**645**	**1206**	**1248**
$36(6 \times 6)$	8748/1741	**910**	**1366**	**1267**
$64(8 \times 8)$	15552/3137	**944**	**1486**	**1299**
$100(10 \times 10)$	24300/4941	**868**	**1495**	**1881**

Source: own elaboration

Tab. 37.3 $\mathbf{D}_F = abs(diag(\mathbf{F}))$

s	$primal/dual$	$g = 0.05$	$g = 10$	$g = 40$
$4(2 \times 2)$	972/173	**307**	**415**	**332**
$16(4 \times 4)$	3888/753	**374**	**570**	**531**
$36(6 \times 6)$	8748/1741	**448**	**586**	**564**
$64(8 \times 8)$	15552/3137	**429**	**666**	**617**
$100(10 \times 10)$	24300/4941	**464**	**837**	**604**

Source: own elaboration

Tab. 37.4 $\mathbf{D}_F = diag(\mathbf{F})$

s	$primal/dual$	$g = 0.05$	$g = 10$	$g = 40$
$4(2 \times 2)$	972/173	**142**	**223**	**181**
$16(4 \times 4)$	3888/753	**181**	**255**	**247**
$36(6 \times 6)$	8748/1741	**192**	**267**	**263**
$64(8 \times 8)$	15552/3137	**187**	**326**	**257**
$100(10 \times 10)$	24300/4941	**189**	**339**	**346**

Source: own elaboration

Example 2. In Table 37.5–Table 37.8 we test the efficiency of the same preconditioners as in Example 1 for the fixed number of subdomains $s = 16(4 \times 4)$ and changing H/h. The conclusion is analogous.

Tab. 37.5 $\mathbf{D}_F = \mathbf{I}$

H/h	$primal/dual$	$g = 0.05$	$g = 10$	$g = 40$
2	432/225	**607**	**660**	**855**
4	1200/401	**660**	**1006**	**944**
8	3888/753	**717**	**1205**	**1292**
16	13872/1457	**1277**	**1447**	**1381**

Source: own elaboration

Tab. 37.6 $\mathbf{D}_F = d \times \mathbf{I}$ **with** $d = (f_{\max} + f^+_{\min})/2$

H/h	$primal/dual$	$g = 0.05$	$g = 10$	$g = 40$
2	432/225	**613**	**672**	**861**
4	1200/401	**678**	**1002**	**951**
8	3888/753	**645**	**1206**	**1248**
16	13872/1457	**925**	**1545**	**1385**

Source: own elaboration

Tab. 37.7 $\mathbf{D}_F = abs(diag(\mathbf{F}))$

H/h	$primal/dual$	$g = 0.05$	$g = 10$	$g = 40$
2	432/225	**274**	**422**	**380**
4	1200/401	**300**	**540**	**407**
8	3888/753	**374**	**570**	**531**
16	13872/1457	**584**	**762**	**782**

Source: own elaboration

Tab. 37.8 $\mathbf{D}_F = diag(\mathbf{F})$

H/h	$primal/dual$	$g = 0.05$	$g = 10$	$g = 40$
2	432/225	**171**	**209**	**195**
4	1200/401	**160**	**240**	**191**
8	3888/753	**181**	**255**	**247**
16	13872/1457	**213**	**371**	**306**

Source: own elaboration

Example 3. In Table 37.9 we report informations on diagonal entries of $\mathbf{D}_F = diag(\mathbf{F}) = (d_{ii})$. The symbols n^-, n^+ stand for the number of the negative, positive diagonal entries, respectively. Their extremal values are denoted as follows: $d_{\min} = \min\{d_{ii}\}$, $d_{\max} = \max\{d_{ii}\}$, $d^-_{\max} = \max\{d_{ii} : d_{ii} \leq 0\}$, and $d^+_{\min} = \min\{d_{ii} : d_{ii} \geq 0\}$.

Tab. 37.9 $\mathbf{D}_F = diag(\mathbf{F})$

s	$primal/dual$	n^-	$d_{\min}$	$d^-_{\max}$	n^+	$d^+_{\min}$	$d_{\max}$
$4(2 \times 2)$	972/173	35	−6686.73	−2992.82	138	0.51	2.98
$16(4 \times 4)$	3888/753	207	−26845.36	−11194.80	546	0.46	3.11
$36(6 \times 6)$	8748/1741	515	−61182.94	−24389.52	1226	0.45	3.15
$64(8 \times 8)$	15552/3137	959	−108974.69	−42644.74	2178	0.45	3.17
$100(10 \times 10)$	24300/4941	1539	−170825.04	−65962.02	3402	0.44	3.19

Source: own elaboration

CONCLUSION

The path-following interior point algorithm was used for solving the Stokes problem with the stick-slip boundary condition. The inner linear systems was solved by the preconditioned projected conjugate gradient method with the oblique projector as the preconditioner. Its definition depends on the choice of a diagonal matrix. It was experimentally shown that the diagonal of the dual Hessian leads to the best performance of computations. It is relatively surprising, since it contains the negative diagonal entries and it is not positive definite, as it is required by theory.

ACKNOWLEDGMENTS

This research was supported by The Ministry of Education, Youth and Sports from the National Programme of Sustainability (NPU II) project "IT4Innovations excellence in science - LQ1602" and from the Large Infrastructures for Research, Experimental Development and Innovations project „IT4Innovations National Supercomputing Center – LM2015070" and by the project No. 17-01747S of the Czech Science Foundation.

REFERENCES

1. C. L. M. H. Navier. "Mémoire sur les lois du movement des fluides", Mém. de l Acad. R. Sci. Paris, 1823, 6: 389416.
2. I. J. Rao, K. Rajagopal. "The effect of the slip boundary condition on the flow of fluids in a channel", *Acta Mechanica*, Vol. 135(3), 1999, p. 113–126.
3. M. Ayadi, L. Baffico, M. K. Gdoura, T. Sassi. "Error estimates for Stokes problem with Tresca friction conditions", *ESAIM: Math. Model. Numer. Anal.*, Vol. 48(5), 2014, p. 1413–1429.
4. D. Arnold, F. Brezzi, M. Fortin. "A stable finite element for the stokes equations", Calcolo, 21(4), 1984, p. 337–344.
5. J. Koko. "Vectorized Matlab codes for the Stokes problem with P1-bubble/P1 finite element", 2012, *http://www.isima.fr/˜ jkoko/Codes/StokesP1BubbleP1.pdf* [online].
6. Z. Dostál, D. Horák, R. Kučera. "Total FETI - an easier implementable variant of the FETI method for numerical solution of elliptic PDE", *Commun. Numer. Methods Eng.*, Vol. 22(12), 2006, p. 1155–1162.
7. R. Kučera, J. Machalová, H. Netuka, P. Ženčák. "An interior point algorithm for the minimization arising from 3D contact problems with friction", *Optim. Methods Softw.*, 6(28), 2013, p. 1195–1217.
8. R. Kučera, V. Šátek, M. Jarošová. "Path-following interior point method for QPP with box and equality constraints: theory and applications", in preparation 2017.

9. R. Kučera, J. Haslinger, V. Šátek, M. Jarošová. "Efficient methods for solving the Stokes problem with slip boundary conditions", *Math. Comput. Simul.*, http://dx.doi.org/10.1016/j.matcom.2016.05.012.
10. M. Jarošová, R. Kučera, V. Šátek. "A new variant of the path-following algorithm for the parallel solving of the Stokes problem with friction", in P. Iványi, B. H. V. Topping (Editors), *Proceedings of the Fourth International Conference on Parallel, Distributed, Grid and Cloud Computing for Engineering*. Civil-Comp Press, Paper 11, Stirlingshire, UK, 2015.
11. R. Kučera, T. Kozubek, A. Markopoulos. "On large-scale generalized inverses in solving two-by-two block linear systems", *Linear Algebra Appl.*, 438(7), 2013, p. 3011–3029.

PRECONDITIONING IN THE PATH-FOLLOWING ALGORITHM FOR THE STOKES FLOW WITH STICK-SLIP CONDITIONS

Abstract: *The Stokes problem with the stick-slip boundary condition is solved by the mixed finite element method combined with the TFETI method. An interior point method for the minimization subject to box and equality constraints is used. The preconditioned projected conjugate gradient method solves the inner linear systems. The preconditioners are tested experimentally. The aim of our research is to develop efficient solvers for modelling of a flow over hydrophobic walls that exhibits applications in engineering areas including biomedical modelling or transport of fluid.*

Keywords: *Stokes problem; stick-slip condition; interior point method; TFETI method.*

PŘEDPODMÍNĚNÍ ALGORITMU SLEDOVÁNÍ CESTY PRO STOKESOVO PROUDĚNÍ SE SKLUZOVOU PODMÍNKOU

Abstrakt: *Stokesova úloha se skluzovou podmínkou je řešena smíšenou metodou konečných prvků kombinovanou s TFETI metodou. Výpočet řešení se provádí metodou vnitřních bodů určenou k minimalizaci s oboustraným omezením a rovnostní vazbou. Předpodmíněná projektovaná metoda sdružených gradientů se používá pro řešení vnitřních lineárních soustav. Účinost předpodmiňovačů se testuje experimentálně. Cílem výzkumu je vyvinout efektivní řešiče pro modelování proudění po hydrofobních stěnách, což nachází uplatnění v inženýrských oblastech zahrnujících modelování v biomedicíně nebo při přenosu tekutin.*

Klíčová slova: *Stokesova úloha; skluzová podmínka; metoda vnitřních bodů; TFETI metoda.*

Date of submission of the article to the Editor: 04.2017
Date of acceptance of the article by the Editor: 05.2017

Ing. Marta JAROŠOVÁ, Ph.D.
VŠB - Technical University of Ostrava
IT4Innovations
17. listopadu 15/2172, 708 33, Ostrava, Czech Republic
tel.: +420 597 329 120, e-mail: marta.jarosova@vsb.cz

doc. RNDr. Radek KUČERA, Ph.D.
VŠB - Technical University of Ostrava
Department of Mathematics and Descriptive Geometry
17. listopadu 15/2172, 708 33, Ostrava, Czech Republic
tel.: +420 597 324 126, e-mail: radek.kucera@vsb.cz

Ing. Václav ŠÁTEK, Ph.D.
VŠB - Technical University of Ostrava
IT4Innovations
17. listopadu 15/2172, 708 33, Ostrava, Czech Republic
tel.: +420 597 329 120, e-mail: vaclav.satek@vsb.cz